

Particle decay branching ratios for states of astrophysical importance in ^{19}Ne

D. W. Visser,* J. A. Caggiano, R. Lewis, W. B. Handler,† A. Parikh, and P. D. Parker
A. W. Wright Nuclear Structure Laboratory, Yale University, New Haven, Connecticut 06520-8124
(Dated: October 25, 2018)

We have measured proton and alpha-particle branching ratios of states formed using the $^{19}\text{F}(^3\text{He},t)^{19}\text{Ne}^*$ reaction at a beam energy of 25 MeV. These ratios have a large impact on the astrophysical reaction rates of $^{15}\text{O}(\alpha,\gamma)^{19}\text{Ne}$, $^{18}\text{F}(p,\gamma)^{19}\text{Ne}$ and $^{18}\text{F}(p,\alpha)^{15}\text{O}$, which are of interest in understanding energy generation in x-ray bursts and in interpreting anticipated γ -ray observations of novae. We detected decay protons and alpha particles using a silicon detector array in coincidence with tritons measured in the focal plane detector of our Enge split-pole spectrograph. The silicon array consists of five strip detectors of the type used in the Louvain-Edinburgh Detector Array, subtending angles from 130° to 165° with approximately 14% lab efficiency. The correlation angular distributions give additional confidence in some prior spin-parity assignments that were based on gamma branchings. We measure $\Gamma_p/\Gamma = 0.387 \pm 0.016$ for the 665 keV proton resonance, which agrees well with the direct measurement of Bardayan *et al.*.

PACS numbers: 26.30.+k, 26.50.+x, 27.20.+n

I. INTRODUCTION

States in ^{19}Ne corresponding to $^{15}\text{O}+\alpha$ ($Q_{\alpha\gamma}=3529.4$ keV) and $^{18}\text{F}+p$ ($Q_{p\gamma}=6411.2$ keV) resonances play an important role in explosive hydrogen burning. In energetic events known as x-ray bursts, $^{15}\text{O}(\alpha,\gamma)^{19}\text{Ne}$ has long been thought to be a possible pathway from the hotCNO energy-generation bottleneck into the more exoergic hydrogen-burning processes above $A=19$, such as the NeNa cycle and the rp process [1]. In novae, the β^+ decay of ^{18}F is expected to be the prime source of the 511 keV γ -ray line, and of the sub-511-keV continuum γ -ray flux, observable by orbiting γ -ray observatories such as INTEGRAL [2]. The final yield of ^{18}F and its associated radiation is sensitive to the reaction rates of $^{18}\text{F}(p,\gamma)^{19}\text{Ne}$ and $^{18}\text{F}(p,\alpha)^{15}\text{O}$ [3, 4].

The level density at relevant energies above the proton and alpha thresholds is low, so that the nuclear reactions mostly take place through isolated and narrow resonances. The temperature-dependent resonant reaction rates may be calculated by summing over resonances [5]:

$$\langle \sigma v \rangle = \sum_R \left(\frac{2\pi}{\mu kT} \right)^{3/2} \hbar^2 (\omega\gamma)_R \exp\left(-\frac{E_R}{kT}\right), \quad (1)$$

where μ is the reduced mass, k is Boltzmann's constant, T is the temperature, E_R is the resonance energy and $\omega\gamma$ is its strength. The first factor in the resonance strength, ω , is a statistical factor that depends on the spins in the incoming and outgoing channel, while γ depends on the

width and branching ratios for the resonance:

$$\gamma = \frac{\Gamma_a \Gamma_b}{\Gamma} \Gamma, \quad (2)$$

where a and b denote the incoming and outgoing particles (p , α or γ) for the reaction $I(a,b)F$. Thus, the reaction rate has a linear dependence on the branching ratios.

II. EXPERIMENT

Previous experiments have measured astrophysically-important branching ratios [6, 7, 8, 9, 10] and resonance strengths [11, 12, 13, 14] for ^{19}Ne . The goal of the present experiment was to perform an independent measurement of these branching ratios, and to achieve higher sensitivity in that measurement by using large-area silicon strip detectors [15]. These detectors provided a large solid angle and an angular resolution in the lab of approximately 2° [16].

The $^{19}\text{F}(^3\text{He},t)^{19}\text{Ne}$ reaction was studied using 25 MeV ^3He beams provided by the WNSL ESTU tandem Van de Graaf accelerator. The beam, with a typical current of 19 pA, was incident on $80 \mu\text{g}/\text{cm}^2$ of CaF_2 deposited on a $10 \mu\text{g}/\text{cm}^2$ carbon foil. The Enge spectrograph was placed at $\theta = 0^\circ$ with an aperture solid angle of 12.8 msr, and reaction products were momentum analyzed using a magnetic field of approximately 12.9 kG. The focal plane detector [17] measured the position (momentum), horizontal angle, ΔE (energy loss in isobutane) and E (energy loss in a plastic scintillator). Particle identification (PID) was accomplished mainly by a gate on energy vs. momentum. Gates on other 2-d event plots further refined the PID. Tritons were easily distinguished from the only other incident particles, deuterons. The horizontal tracking information was used to correct the dominant ($x|\Theta^3$) aberration in the spectrograph's focussing.

Protons and alpha particles from the decay of unbound states were detected by the Yale Lamp Shade Array

*Present address: Physics Division, Oak Ridge National Laboratory, Oak Ridge, Tennessee 37831; Electronic address: dale.visser@mailaps.org

†Present address: Physics and Astronomy Department, University of Western Ontario, London, Ontario, Canada N6A 3K7

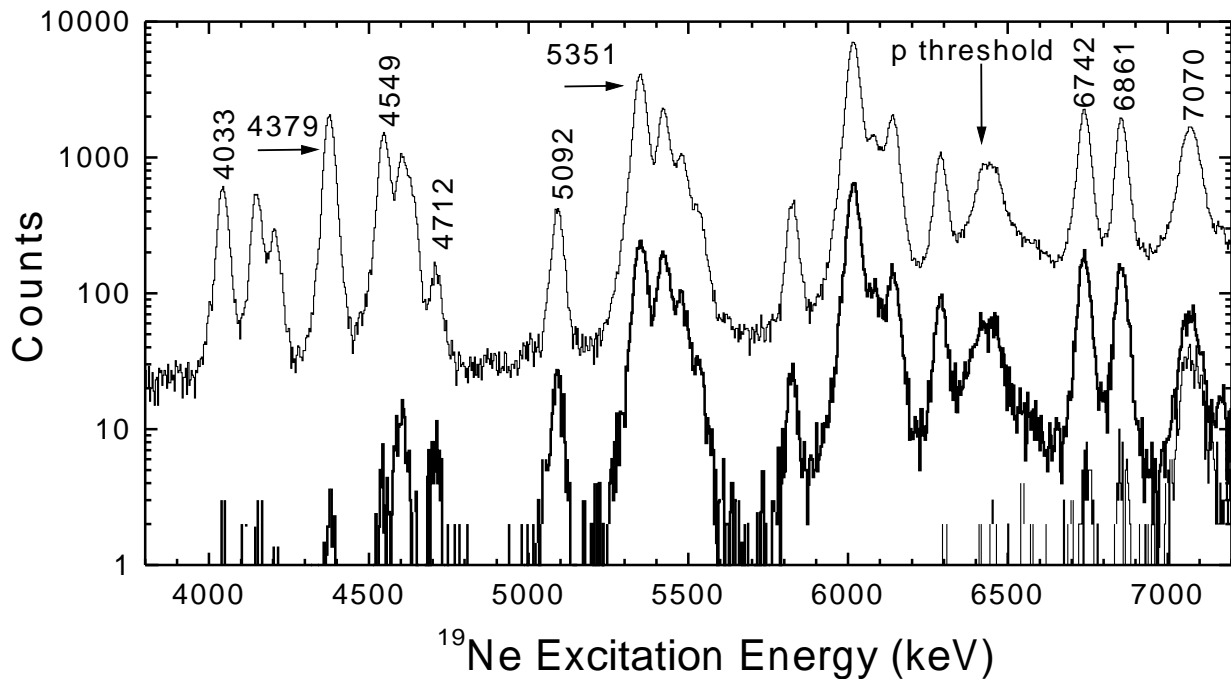


FIG. 1: The top curve is the triton spectrum from data set D4, with the abscissa transformed to show ^{19}Ne excitation energy. The darker middle curve shows the tritons coincident with alpha-particles in YLSA, while the lower curve shows candidate events for tritons coincident with protons in YLSA, i.e., random contributions are not subtracted. The $^{15}\text{O}+\alpha$ threshold lies at $E_x=3529.4$ keV.

(YLSA), an array constructed from five sectors of silicon strip detectors of the type used in the Louvain-Edinburgh Detector Array [15]. The segments were arranged in an axially-symmetric 5-sided “lamp shade” configuration covering angles from $\theta = 130^\circ$ to $\theta = 165^\circ$, with approximately 14% lab efficiency. The detectors were approximately $500\ \mu\text{m}$ thick; a bias voltage of 100 V was applied to them. Since it was essential that the beam go through the center of the chamber, two collimators were used for tuning: one at the entrance and one at the exit of the scattering chamber; both were 2 mm in diameter. YLSA was protected from particles scattered off the up- and downstream collimators by the detector mount and an aluminum sheet, respectively [18]. After tuning, these collimators were rotated out of the beam path.

In order to ensure proper functioning of the silicon detectors in the environment of electrons ejected from the target by the relatively intense beam, the sides of the detectors closest to the strips’ pn-junctions, which have exposed SiO_2 between them, faced away from the target. Also, the target had strong rare-earth magnets immediately to either side to deflect electrons, and the target ladder, aluminum sheet and detector mount were biased with +500 V to attract electrons away from the detector [18].

A fast trigger was produced by the scintillator in the spectrograph’s focal plane detector. Uninteresting events were discarded using rough PID based on the ΔE and E signals. The “fast-clear” (FCLR) feature of the CAEN

V785/V775 ADC’s and TDC’s was used for this hardware cut, and did not reliably clear all modules at high trigger rates. This was undiscovered until after the measurement was made, resulting in the need for efficiency corrections. Fast discriminators on each of the 80 (5×16) silicon detector channels produced logic pulses which were passed through fixed 300-nsec delays to produce time spectra. Decay protons were distinguished from decay alpha particles by their differing energies.

Once PID was used to select the ($^3\text{He},t$) channel and events with possible decay energies were extracted from the data, the momentum spectrum of coincident decays (see Fig. 1) was determined by requiring the time to lie within the peak in the time spectrum. A background spectrum was produced using candidate events with measured times outside the peak. This background spectrum was used to quantify the rate of random coincidences.

The energy calibration for YLSA was determined using a ^{228}Th alpha-particle source. The exact location of the discriminator thresholds varied by strip and was uncertain. The detectors in YLSA have an estimated 2- μm dead layer; in simulations, deposited energies for alpha particles incident on YLSA ranged from 300 to 600 keV, depending on lab angle and the angle of incidence. Because of this, the lowest $^{15}\text{O} + \alpha$ resonance for which a reliable branching ratio could be extracted was at $E_R=1020$ keV ($E_x=4549$ keV). Likewise, the only $^{18}\text{F}+p$ resonance with a reliable proton branching ratio was $E_R=665$ keV ($E_x=7076$ keV). Above $E_x=7076$ keV,

the triton energy calibration was uncertain, and states were not well resolved from one another.

III. SIMULTANEOUS FIT OF THE DATA SETS

Since all spherical harmonics with non-zero magnetic substates are suppressed at $\theta = 0^\circ$, the tritons were detected at $\theta = 0^\circ$ in order to simplify the calculation of the angular correlations. In order to have sufficient counts for fitting, the detected decay particles were divided into four angles (4 strips \times 5 detectors per angle). As in [6], the angular correlation function used for breakup to $^{15}\text{O}_{g.s.}$ was

$$W(\theta) = \sum_{M,m} \left| \langle \frac{1}{2}m; lM - m | JM \rangle Y_l^{M-m}(\theta, \phi) \right|^2, \quad (3)$$

where M are the substates of the ^{19}Ne state with spin J , $p_M = p_{-M}$ are the $J + \frac{1}{2}$ probabilities of substate populations, and $m = \pm \frac{1}{2}$ are the possible magnetic substates of the ^{15}O [21]. For $|M| > \frac{3}{2}$, $p_M \equiv 0$ because the tritons were detected at $\theta = 0^\circ$.

Four separate sets of spectra were analyzed and fit to produce angular distributions. Each set corresponded to a unique set of experimental conditions. Higher ADC thresholds were used in the first data set (D1). The thresholds were lowered for the second and third data sets (D2,D3), which have slightly different energy calibrations from one another. For the fourth data set (D4), the YLSA electronics channels were given a shorter ADC gate than the focal plane channels, in an attempt to reduce pileup in the spectra.

The geometric efficiency of each strip in the array was determined for each resonance using a Monte Carlo simulation of the formation and breakup of the resonances. The $E_x=5351$ keV state is well-populated and has an isotropic c.m. angular distribution for its decay products. It is known to decay almost entirely by alpha-particle emission. (Calculations give $\Gamma_\gamma/\Gamma < 10^{-3}$ [22]; $\omega\gamma = 1.69 \pm 0.14$ eV and $\Gamma = 1.3 \pm 0.5$ keV have been measured for the analog in ^{19}F which is 499 keV closer to its threshold [23].) When measuring the branching ratio for this state, it was found that the result was consistently less than one. The specific result was dependent on the details of the electronics gating. The three different electronics configurations resulted in three different ‘‘coincidence efficiencies’’, ranging from 0.581 ± 0.018 (D4) in the worst case to 0.867 ± 0.027 (D1). For each of the runs, the decay data were divided by this factor.

For $E_x=4379$ keV, the lab energies of the alpha-particles extended below the thresholds for the detector. The exact energy of these thresholds varies with detector strip and is not precisely known. If one (falsely) assumes that all decay alpha particles were detected for this state, a 90% confidence interval for Γ_α/Γ of (0.0027,0.0143) is found. This is interpreted as meaning $\Gamma_\alpha/\Gamma > 0.0027$ with a probability greater than 90%. Lower limits of

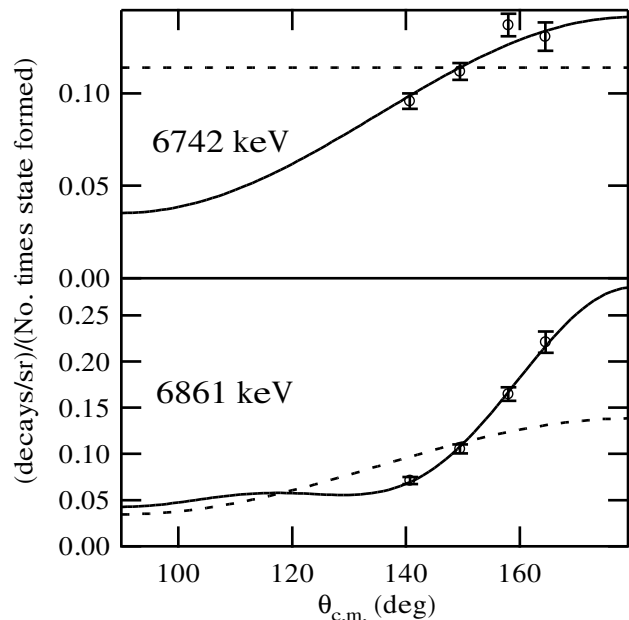


FIG. 2: Angular distributions of decay alpha-particles. (a) $E_x=6742$ keV, solid curve for $J^\pi=\frac{3}{2}^-$, dashed curve for $J^\pi=\frac{1}{2}^-$. (b) $E_x=6861$ keV, solid curve for $J^\pi=\frac{7}{2}^-$, dashed curve for $J^\pi=\frac{3}{2}^-$.

0.003 and 0.007 for Γ_p/Γ of the $E_x=6742$ and 6861 keV states, respectively, were determined in the same way. In these latter two cases, only data set D4 supports a non-zero result, which is cause for skepticism, especially since calculations based on the measured mirror state in ^{19}F [7] and a direct measurement of $\Gamma_p=2.22 \pm 0.69$ eV [14] estimate $\Gamma_p/\Gamma=8.2 \times 10^{-4}$ for the $E_x=6742$ keV state [7]. The ratio extracted from D4 is significantly different only for these two states.

As can be seen in Fig. 1, the energy (E_x) resolution of the triton spectrum was about 40 keV, so the peaks for the states at $E_x=4600$ and 4635 keV were not well resolved. Since the $E_x=4635$ keV state is not expected to emit significant numbers of alpha-particles (due to its $l = 7$ angular momentum barrier), in our analysis of the coincidence data for these two states we attributed all of the measured decay alpha-particles to the $E_x=4600$ keV state.

For the 330-keV proton resonance at $E_x=6742$ keV, we measured the spin and parity using the angular distribution of its decay alpha-particles. The $^{20}\text{Ne}(^3\text{He},\alpha)^{19}\text{Ne}$ angular distribution measured for this state shows $l = 1$ character, implying negative parity and $J = \frac{1}{2}$ or $\frac{3}{2}$ [24]. $J^\pi = \frac{1}{2}^-$ would imply an isotropic correlation function for the decay alpha-particles, but Fig. 2a shows that $J^\pi = \frac{3}{2}^-$ results in a much better fit to the data.

A previous high-resolution measurement has shown that the ($^3\text{He},t$) reaction populates the 450 keV proton resonance [7], and not an $l = 1$ resonance (isospin mirror of the $J^\pi=\frac{3}{2}^-$, $E_x=6891$ keV state in ^{19}F) predicted to

TABLE I: Branching ratio results below the proton threshold, with error bars given at a 68.27% confidence level. Unless otherwise stated, J^π assignments are from [19].

E_x [keV]	E_R [keV]	J^π	Γ_α/Γ^a	Γ_α/Γ [6]	other Γ_α/Γ	Γ_α/Γ [10]	Γ_α/Γ (Average)
4379	850	$7/2^+$	$(>0.0027)^b$	0.044 ± 0.032	0.016 ± 0.005 [9]	$<0.0039^c$	
4549	1020	$(1/2^-)$ [20]	0.06 ± 0.04	0.07 ± 0.03		0.16 ± 0.04	0.09 ± 0.04
4600	1071	$3/2^-$	0.208 ± 0.026^d	0.25 ± 0.04	0.32 ± 0.03 [8]	0.32 ± 0.04	0.27 ± 0.05
4712	1183	$(5/2^-)$	$0.69^{+0.11}_{-0.14}$	0.82 ± 0.15		0.85 ± 0.04	0.83 ± 0.05
5092	1563	$5/2^+$	$0.75^{+0.06}_{-0.07}$	0.90 ± 0.09	0.80 ± 0.10 [9]	0.90 ± 0.05	0.84 ± 0.07

^aThis work.

^bTentative. See text for details.

^c90% confidence.

^dUnresolved with $E_x=4635$ keV. See text for details.

TABLE II: Branching ratio measurements above the proton threshold.

E_x [keV]	E_R [keV]	J^π	Γ_α/Γ^a	Γ_α/Γ [7]	Γ_α/Γ (Average)	Γ_p/Γ^a	Γ_p/Γ [7]	Γ_p/Γ (Average)
6742	330	$3/2^-$	$0.901^{+0.074}_{-0.031}$	1.04 ± 0.08	$0.96^{+0.07}_{-0.04}$	$(>0.003)^b$		
6861	450	$7/2^-$	$0.932^{+0.028}_{-0.031}$	0.96 ± 0.08	$0.935^{+0.026}_{-0.029}$	$(>0.007)^b$	<0.025	
7076	665	$3/2^+$ [11, 12, 13]	0.613^c	0.64 ± 0.06		0.387 ± 0.016	0.37 ± 0.04	0.385 ± 0.015

^aThis work.

^bTentative. See text for details.

^cSimultaneous fit assumed $\Gamma = \Gamma_\alpha + \Gamma_p$.

lie near 430 keV [25]. The decay alpha-particle angular distribution in Fig. 2b shows that a spin assignment of $\frac{7}{2}^-$ is the appropriate choice for the peak at this location in our spectrum.

The measurement of $\Gamma_p/\Gamma = 0.387\pm 0.016$ for the 665-keV proton resonance is in agreement with the previously measured value [7]. It disagrees with the branching ratio implied by the direct measurement performed at Louvain-la-Neuve [11], but agrees with the measurements made at Oak Ridge National Laboratory [13].

IV. CONCLUSIONS

The branching ratio measurements presented here are compared with previous measurements in Tables I and II. In cases where other measured values exist, weighted

averages are given. The measurement provides support for the $J^\pi = \frac{3}{2}^-$ assignment for the 330-keV $^{18}\text{F}(p,\gamma)$ resonance, which dominates the reaction rate above 450 MK [7]. The 450-keV $^{18}\text{F}+p$ resonance is also confirmed to have $J^\pi = \frac{7}{2}^-$, re-affirming its weak role in astrophysical processes [7]. The measured branching ratio for the 665-keV $^{18}\text{F}+p$ resonance, which strongly affects both $^{18}\text{F}(p,\gamma)$ and $^{18}\text{F}(p,\alpha)$ astrophysical rates [7], differs from one recent direct measurement [11] and agrees with another [13]. Therefore, these reaction rates can now be calculated with greater confidence.

V. ACKNOWLEDGEMENTS

This work was supported under US Department of Energy Grant No.DE-FG02-91ER-40609.

- [1] M. Wiescher, J. Görres, and H. Schatz, J. Phys. G: Nucl. Part. Phys. **25**, R133 (1999).
- [2] M. Hernanz, J. José, A. Coc, J. Gómez-Gomar, and J. Isern, Astrophys. J. **526**, L97 (1999).
- [3] A. Coc, M. Hernanz, J. José, and J.-P. Thibaud, Astron. & Astrophys. **357**, 561 (2000).
- [4] C. Iliadis, A. Champagne, J. José, S. Starrfield, and P. Tupper, Astrophys. J. Suppl. **142**, 105 (2002).
- [5] C. E. Rolfs and W. S. Rodney, *Cauldrons in the Cosmos* (The University of Chicago, Chicago, 1988).
- [6] P. V. Magnus, M. S. Smith, A. J. Howard, P. D. Parker,

- and A. E. Champagne, Nucl. Phys. **A506**, 332 (1990).
- [7] S. Utku, J. G. Ross, N. P. T. Bateman, D. W. Bardayan, A. A. Chen, J. Görres, A. J. Howard, C. Iliadis, P. D. Parker, M. S. Smith, et al., Phys. Rev. C **57**, 2731 (1998), and Phys. Rev. C **58** (1998) 1354e.
- [8] A. M. Laird, S. Cherubini, A. N. Ostrowski, M. Aliotta, T. Davinson, A. D. Pietro, P. Figuera, W. Galster, J. S. Graulich, D. Groombridge, et al., Phys. Rev. C **66**, 048801 (2002).
- [9] K. E. Rehm, A. H. Wuosmaa, C. L. Jiang, J. Caggiano, J. P. Greene, A. Heinz, D. Henderson, R. V. F. Janssens,

- E. F. Moore, G. Mukherjee, et al., Phys. Rev. C **67**, 065809 (2003).
- [10] B. Davids, A. M. van den Berg, P. Dendooven, F. Fleurot, M. Hunyadi, M. A. de Huu, K. E. Rehm, R. E. Segel, R. H. Siemssen, H. W. Wilschut, et al., Phys. Rev. C **67**, 012801 (2003).
- [11] J. S. Graulich, S. Cherubini, R. Coszach, S. E. Haffami, W. Galster, and P. Leleux, Phys. Rev. C **63**, 011302R (2000).
- [12] K. E. Rehm, K. Paul, A. D. Roberts, C. L. Liang, D. J. Blumenthal, S. M. Fischer, J. Gehring, D. Henderson, J. Nickles, J. Nolen, et al., Phys. Rev. C **53**, 1950 (1996).
- [13] D. W. Bardayan, J. C. Blackmon, W. Bradfield-Smith, C. R. Brune, A. E. Champagne, T. Davinson, B. A. Johnson, R. L. Kozub, C. S. Lee, R. Lewis, et al., Phys. Rev. C **63**, 065802 (2001).
- [14] D. W. Bardayan, J. C. Batchelder, J. C. Blackmon, A. E. Champagne, T. Davinson, R. Fitzgerald, W. R. Hix, C. Iliadis, R. L. Kozub, Z. Ma, et al., Phys. Rev. Lett. **89**, 262501 (2002).
- [15] T. Davinson, W. Bradfield-Smith, S. Cherubini, A. DiPietro, W. Galster, A. M. Laird, P. Leleux, A. Ninane, A. N. Ostrowski, A. C. Shotter, et al., Nucl. Inst. & Meth. A **454**, 350 (2000).
- [16] D. W. Visser, Ph.D. thesis, Yale University (2003).
- [17] A. A. Chen, R. Lewis, K. B. Swartz, D. W. Visser, and P. D. Parker, Phys. Rev. C **63**, 065807 (2001).
- [18] W. Bradfield-Smith, R. Lewis, P. D. Parker, and D. W. Visser, Nucl. Inst. & Meth. A **481**, 183 (2002).
- [19] D. R. Tilley, H. R. Weller, C. Cheves, and R. Chasteler, Nucl. Phys. **A595**, 1 (1995), updated revised manuscript 9 November 2000.
- [20] J. M. Davidson and M. L. Roush, Nucl. Phys. **A213** (1973).
- [21] G. R. Satchler, *Introduction to Nuclear Reactions* (J. Wiley, New York, 1980).
- [22] K. Langanke, M. Wiescher, W. A. Fowler, and J. Görres, Astrophys. J. **301**, 629 (1986).
- [23] S. Wilmes, V. Wilmes, G. Staudt, P. Mohr, and J. W. Hammer, Phys. Rev. C **66**, 065802 (2002).
- [24] J. D. Garrett, R. Middleton, and H. T. Fortune, Phys. Rev. C **2**, 1243 (1970).
- [25] N. Shu, D. W. Bardayan, J. C. Blackmon, Y. S. Chen, R. L. Kozub, P. D. Parker, and M. S. Smith, Chinese Phys. Lett. (2003), accepted.